Karson, J.A., Cannat, M., Miller, D.J., and Elthon, D. (Eds.), 1997
Proceedings of the Ocean Drilling Program, Scientific Results, Vol. 153

26. *DATA REPORT:* GEOCHEMISTRY AND MINERAL CHEMISTRY OF ULTRAMAFIC ROCKS FROM THE KANE AREA (MARK)[1]

Carl-Dietrich Werner[2] and Joachim Pilot[2]

ABSTRACT

A suite of serpentinized peridotites from Leg 153 was analyzed for major and trace elements. All the rocks are less-refractory peridotites. The mineral chemistry of olivines (Mg# = 90.3), orthopyroxenes (Mg# = 90.4), clinopyroxenes (Mg# = 91.6), and some Cr spinels (Mg# = 68.4; Cr# = 29.7) shows the characteristic features of minerals from less-depleted mantle peridotites. Some geothermometric calculations gave temperatures for the pyroxene system of about 1300°C, reflecting the prekinematic to synkinematic crystallization of the pyroxenes, and gave a range from 1180° to 1075°C for the mineral pair orthopyroxene and spinel. Oxygen-isotope determinations show $\delta^{18}O$ values of about 6‰ for olivine, orthopyroxene, and clinopyroxene; $\delta^{18}O$ values from chromian spinel/magnetite vary between 2.9‰ and 3.8‰, values from serpentine vary between 2.8‰ and 5.3‰, and whole-rock values vary between 2.9‰ and 4.6‰. Two temperatures could be calculated from the oxygen-isotope exchange for the mineral pair clinopyroxene and spinel: about 1100° and about 900°C. The 1100°C value nearly corresponds to the data obtained using the orthopyroxene-spinel mineral thermometer, and may indicate subsolidus deformation and recrystallization. The temperature range of the serpentinization could only be estimated. It depends upon the rock/water ratio, and may not have exceeded ~300°C. Finally, a calculation of possible rock/water ratios is given.

INTRODUCTION

Serpentinized peridotites are exposed in a belt about 2 km wide and more than 20 km long on the western median valley wall of the Mid-Atlantic Ridge south of the Kane Fracture Zone (MARK) at 23°20′ N. This outcrop is interpreted as a part of the oceanic upper mantle uplifted during tectonic extension of the slowly spreading Mid-Atlantic Ridge (Cannat et al., 1995; Karson and Winters, 1992; Purdy and Detrick, 1986).

Shipboard documentation has shown that the ultramafic complex from Site 920 (Leg 153) can be divided into several "units," which differ especially in their fabrics and slightly in their degrees of serpentinization. All samples are moderately to strongly serpentinized harzburgites with 15%–30% relict minerals (Cannat, Karson, Miller, et al., 1995).

Polished thin sections were used for microscope investigations and also for microprobe work, which was conducted on the "CAMEBAX S 50" at the Ruhr Universität, Bochum.

Major-element oxides and trace elements (Ga, Pb, Cu, Zn, Y, Nb, Zr, Ti, V, Ni, Co, Cr, Sc, S, and Cl) were measured by X-ray fluorescence spectroscopy (XRF) using a Philips PW 1480 sequential spectrometer. The XRF was used to analyze both pressed pellets and glass discs prepared from powdered, but not ignited, material with lithium tetraborate. Na, K, Li, Rb, and Zn were analyzed by flame photometry, Sr and Ba by inductively coupled plasma-atomic emission spectroscopy (ICP-AAS) using a Perkin-Elmer PLASMA 1000 spectrometer, and As and Sb by inductively coupled plasma-mass spectrometry (ICP-MS) using a Perkin-Elmer ELAN 5000 spectrometer. Boron was determined by optical spectroscopy, with boron-free spectral carbons, using a Carl Zeiss PGS 2 spectrograph.

$\delta^{18}O$ was determined from whole-rock samples and from mineral separates of olivine, orthopyroxene, clinopyroxene, serpentine, and chromian spinel/magnetite.

SAMPLE MATERIAL

Two samples from Hole 920B and 8 samples from Hole 920D, together with an Ocean Drilling Program (ODP) internal laboratory standard ("Ultra"), were chosen for geochemical investigation. Two further samples from Hole 920D were used only for microprobe investigations. The special sample designations correspond to the shipboard documentation (Cannat, Karson, Miller, et al., 1995), but simpler numbers, defined in Table 1, are used in most of the tables and parts of the text.

WHOLE-ROCK GEOCHEMISTRY

The results of the chemical investigations are compiled in Table 2. The CIPW (after the authors Cross, Iddings, Pearson, Washington) norm calculations (converted to 100% and with total Fe as Fe^{2+}) are listed in Table 3. Generally, the chemical and mineralogical compositions of the investigated ultramafic rocks are within the ranges previously reported for the Kane region by Aumento and Loubat (1971), Cannat et al. (1992), Dick et al. (1984), Michael and Bonatti (1985), and Miyashiro et al. (1969). The chemical and mineralogical data show the characteristic features of serpentinized harzburgitic ultra-

Table 1. Identification of sample numbers.

Sample number	Hole, core, section, piece	Depth (mbsf)
1	920B-8R-4, Piece 11	75.5
2	902B-13R-1, Piece 2C	117.6
5	920D-3R-1, Piece 6	18.2
6	920D-5R-1, Piece 4	37.1
8	920D-14R-4, Piece 6	119.4
10	920D-16R-1, Piece 5D	134.4
11	920D-16R-6, Piece 10	140.3
12	920D-19R-1, Piece 5	162.7
13	920D-20R-5, Piece 4	177.6
14	920D-21R-2, Piece 5B	183.9
15	920D-22R-2, Piece 1D	192.1
16	920D-22R-4, Piece 1B	193.7

[1]Karson, J.A., Cannat, M., Miller, D.J., and Elthon, D. (Eds.), 1997. *Proc. ODP, Sci. Results,* 153: College Station, TX (Ocean Drilling Program).

[2]TU Bergakademie Freiberg, Institut für Mineralogie, D-09596 Freiberg, Federal Republic of Germany.

Table 2. Chemical composition of ultramafic rocks from Leg 153.

Sample no.:	1	3	5	6	8	10	12	13	14	16	
Hole:	920B	920B	920D	920D	920D	920D	920D	920D	920D	920D	
Core:	8R	13R	3R	5R	14R	16R	19R	20R	21R	22R	Ultra
Section, piece:	4, 11	1, 2C	1, 6	1, 4	4, 6	1, 5D	1, 5	5, 4	2, 5B	4, 1B	
Depth (mbsf):	75.5	117.6	18.2	37.1	119.4	134.4	162.7	177.6	183.9	193.7	
Major elements (wt%)											
SiO_2	39.5	38.15	38.7	37.9	39.3	38.3	39.0	39.2	38.1	39.4	38.8
TiO_2	0.02	0.011	0.02	0.018	0.008	0.013	0.014	0.024	0.02	0.008	0.02
Al_2O_3	1.13	1.07	1.2	1.21	1.3	1.12	1.26	1.31	1.15	1.2	1.18
Cr_2O_3	0.34	0.35	0.34	0.39	0.38	0.36	0.39	0.37	0.37	0.41	0.365
Fe_2O_3	7.5	7.92	8.15	7.92	8.31	8.09	8.26	7.93	7.95	8.04	8.34
MnO	0.119	0.112	0.087	0.12	0.12	0.11	0.124	0.113	0.12	0.122	0.103
MgO	38.4	38.8	38.5	38.9	38.65	38.7	37.7	37.8	38.8	38.8	37.6
NiO	0.27	0.27	0.27	0.27	0.28	0.29	0.29	0.27	0.28	0.27	0.286
CaO	0.24	0.69	0.14	0.06	0.94	0.83	0.30	0.65	0.35	1.18	0.13
Na_2O	0.09	0.056	0.06	0.06	0.05	0.09	0.07	0.08	0.07	0.08	0.045
K_2O	0.027	0.009	0.032	0.018	0.020	0.009	0.004	0.012	0.012	0.009	0.004
P_2O_5	0.011	0.010	0.010	0.011	0.011	0.011	0.007	0.012	0.010	0.010	0.005
LOI	12.3	12.8	12.5	13.0	10.5	12.2	12.5	12.6	12.7	10.7	13.0
Total	99.95	100.25	100.01	99.88	99.87	100.12	99.92	100.37	99.93	100.23	99.82
Trace elements (ppm)											
B	25	10	24	21	9	5	21	8	24	9	18
Li	5	1	–	–	1	–	1	1	2	2	
Rb	<1	–	–	–	–	–	–	<1	–	~1	–
Sr	2.85	2.89	2.47	0.93	1.45	1.21	4.65	2.28	2.59	2.47	2.24
Ba	0.31	1.62	0.70	0.53	1.25	0.43	0.74	1.01	0.98	0.95	1.9
Ga	–	<1	<2	<2	–	–	<1	–	<2	–	–
Pb	~3	4	4	–	6	~2	5	<2	7	~2	<3
Cu	16	17	24	43	19	27	15	17	21	22	12
Zn	36	38	36	54	47	42	40	37	44	46	40
Y	~1	<1	<1	–	~1	~1	<1	–	<1	–	–
Nb	–	–	~1	<1	<1	–	<1	<1	<1	–	<1
Zr	4	3	~3	3	4	~3	4	4	4	5	3
Ti	120	65	120	110	50	80	85	145	120	50	120
V	46	44	47	48	48	43	48	49	51	48	50
Ni	2150	2135	2105	2130	2180	2250	2250	2145	2205	2150	2250
Co	102	101	98	102	110	108	112	101	99	99	109
Cr	2350	2410	2335	2690	2620	2490	2690	2500	2550	2780	2500
Sc	14	10	11	11	14	11	12	12	8	9	11
S	865	525	890	870	425	540	1050	885	770	380	990
As	0.22	0.71	0.42	0.40	1.38	0.21	2.0	2.3	0.42	1.18	0.71
Sb	0.24	0.25	0.32	0.07	0.34	–	0.04	0.40	0.52	0.22	–
Cl	1095	3795	855	830	2210	2310	1000	2455	1480	2610	735

Notes: – = not detected.

Table 3. CIPW norm of the ultramafic rocks from Leg 153.

Sample no.:	1	3	5	6	8	10	12	13	14	16	Ultra
C	0.63	–	0.96	1.16	–	–	0.69	–	0.48	–	1.06
Or	0.18	0.06	0.22	0.12	0.13	0.06	0.03	0.08	0.08	0.06	0.03
Ab	0.87	0.55	0.59	0.59	0.48	0.87	0.69	0.77	0.69	0.76	0.24
An	1.28	3.05	0.74	0.29	3.68	3.00	1.70	3.61	1.93	3.23	0.71
Opx	27.31	17.71	24.48	21.37	19.82	16.52	26.59	21.33	19.75	18.31	28.73
Cpx	–	0.66	–	–	1.22	1.31	–	–	–	2.61	–
Ol	69.08	77.33	72.36	75.74	73.99	77.27	69.59	73.50	76.37	74.30	68.54
Cm	0.58	0.59	0.58	0.66	0.63	0.91	0.66	0.63	0.63	0.68	0.63
Il	0.04	0.02	0.04	0.04	0.02	0.03	0.02	0.05	0.04	0.02	0.05
Ap	0.03	0.03	0.03	0.03	0.03	0.03	0.03	0.03	0.03	0.03	0.01
TTI	1.05	0.61	0.81	0.71	0.61	0.93	0.72	0.85	0.77	0.82	0.27
An*	60	85	56	33	88	78	71	82	74	81	75
Mg#	90.9	90.5	90.2	90.5	90.1	90.3	89.9	90.5	90.5	90.4	89.8
Ni/Co	21.1	21.1	21.5	20.9	19.8	20.8	20.1	21.2	22.3	21.7	20.6
Cr/Ni	1.09	1.13	1.11	1.26	1.20	1.11	1.20	1.16	1.16	1.29	1.11
Ti/Zr	30	22	40	36	27	26	21	36	30	10	40
Ti/Cr	0.051	0.027	0.051	0.041	0.019	0.032	0.032	0.058	0.047	0.018	0.048
V/Cr	0.020	0.018	0.020	0.018	0.018	0.017	0.018	0.020	0.020	0.017	0.020
Cu/Zn	0.44	0.45	0.67	0.80	0.40	0.64	0.38	0.46	0.48	0.48	0.30

Notes: C = corundum, Or = orthoclase, Ab = albite, An = anorthite, Opx = orthopyroxene, Cpx = clinopyroxene, Ol = olivine, Il = ilmenite, Ap = apatite, An* = normative anorthite content in plagioclase, – = not determined, other abbreviations are defined in the text.

mafic rocks, with Mg# = (Mg/[Mg + Fe]) between 89.8 and 90.9. The Thornton-Tuttle Index (TTI) is generally below 1 (Table 3), and the dominant norm mineral of the H_2O-free calculated rocks is olivine (ca. 70–80 wt%), followed by orthopyroxene (18–29 wt%). Compared to the modal data (between 2 and 5 vol%), normative clinopyroxene contents are generally too low. Plagioclase was not observed in any of the investigated thin sections. Actually, the relatively small amounts of Na, Ca, and Al in normative albite (Ab) and anorthite (An) are incorporated within the pyroxenes, including parts of normative corundum. Another part of Al is a constituent of the spinels.

Geochemical data from our samples suggest a moderate degree of depletion by partial melting, clearly lower than in more northern parts of the Mid-Atlantic Ridge, for instance, the Atlantic or Oceanographer Fracture Zones (Michael and Bonatti, 1985; Dick et al., 1984). The water-free, calculated average of all our analyses (n = 11) is nearly identical to the mean value of analyses from the less-refractory

peridotite of Michael and Bonatti (1985) for the major-element oxides SiO_2, Fe_2O_3, and MgO. This indicates such an insufficient mobility of Si, Fe, and Mg that the bulk chemistry of the protolith was essentially not altered by partial melting and serpentinization. Some minor oxides, however, show lower concentrations in comparison with the Michael and Bonatti (1985), less-refractory peridotite: Cr_2O_3 is 86%, Al_2O_3 is 62%, TiO_2 is 60%, CaO is only 31%, and Na_2O is clearly higher, at 155%. The striking differences among Al_2O_3, CaO, and Na_2O can be explained mainly by serpentinization; this fact is not surprising, because Michael and Bonatti (1985) considered the loss of some components through hydration in their model calculations.

As expected, the data from the three essential oxides (MgO, SiO_2, and Fe_2O_3) show a very low relative variance (V): MgO (V = 1.25%), SiO_2 (V = 1.5%), and Fe_2O_3 (V = 2.95%). The subordinate component Al_2O_3 shows a V = 6.3%. The most variable oxide is CaO (V = 75%), followed by K_2O (V = 64%), TiO_2 (V = 34%), Na_2O (V = 23%), and P_2O_5 (V = 21%). Of the trace elements, Ni, Co, V, and Cr show low variability (V = 2.5%–5.7%). The highest variance values are from Cl (V = 56%), B (48%), S (32%), As and Sb (V ~ 80%), and to Ba, Cu, and Sr (V = 40%–65%). The latter elements were especially influenced by subseafloor metamorphism, which leads to their supply by serpentinization, as for Ca, K, and Na (which are supplied or lost, depending upon the governing temperature conditions, and the varying rock/water relations). Conversely, the concentrations of the compatible elements are very uniform in all of the samples throughout the profile, and even ratios such as Ni/Co, Cr/Ni or V/Cr are very similar (Table 2). However, there is no good correlation between loss on ignition (LOI) and Cl ($r = -0.333$, where r = correlation coefficient). Cl is most probably incorporated in serpentine minerals, whereas Ca was irregularly lost during alteration of clinopyroxene and orthopyroxene. The result of this Ca loss is reflected in the values of the CIPW norm, with only four clinopyroxene-bearing samples (Table 2).

In general, the incompatible-element contents are very low, and are strongly depleted relative to primitive mantle composition (Hofmann, 1988). The following percentages were calculated from averages of 11 ultramafic rocks (Hofmann, 1988): Na = 21%, K = 46%, Sr = 13%, Ba = 16%, Ti = 9%, and Zr = 38%. For instance, an average of 2.4 ppm Sr is much lower than the Sr content of seawater. The depletion of the incompatible elements may result not only from hydration, but also, to a certain extent, from partial melting processes. Obviously, primary deviations in the MARK mantle peridotite composition relative to the worldwide mean composition cannot be ruled out.

MINERAL CHEMISTRY

Olivine

This study dealt only with the relict minerals of samples from Hole 920D. All thin sections investigated contained a comparably high percentage (10–20 vol%) of relatively fresh olivine grains that can be divided into two grain-size groups: (1) elongated, "augen"-like grains, 3–5 mm long, and (2) more or less rounded grains, with a diameter of 1–2 mm.

Both olivine groups are prekinematic or synkinematic. According to Cannat et al. (1992), the elongation is the result of a strong plastic strain with translation, kink banding, and granulation under asthenospheric conditions. Recrystallization of the small grains and their partial kink-band formation, however, occurred in a lower temperature environment.

Microprobe analyses of 83 olivines from both groups (Table 4) show no significant differences in their chemical composition. Forsterite (Fo) varied only between 89.4% and 90.2% or, if $Ni_2(SiO_4)$ is included, between 89.8% and 90.6% (mean values are 89.8% and 90.2%, respectively). Mg# varied between 89.9 and 90.7 (average 90.26). NiO varied between 0.29 wt% and 0.49 wt% (average 0.39 wt%). This variation is considerably higher than that of the MgO content, and was probably caused by internal displacement during tectonic deformation and/or a hydrothermal influence. Some olivine grain profiles show unsystematic patterns: the core can be Ni rich or Ni poor, the rim may show the opposite behavior, but irregular or directed distributions across the grain also occur. FeO, MgO, and MnO, as well as Mg#, show equivalent features. Contents of TiO_2, Al_2O_3, and Cr_2O_3 are very low, and the oxides are sometimes absent altogether. The CaO concentration varies between 0.01 wt% and 0.09 wt%. All of these features are characteristic of olivines from oceanic ultramafic rocks, according to Hamlyn and Bonatti (1980).

The mean values of our olivines (including Mg#) are identical to those reported by Michael and Bonatti (1985) for olivines from less-refractory peridotites from the North Atlantic part of the Mid-Atlantic Ridge, and, therefore, correspond well with the geochemical features of the whole rocks.

The more-refractory olivines from some more northern parts of the Mid-Atlantic Ridge contain higher Fo contents and, therefore, exhibit higher Mg# values. The same is true for olivines from a more southern region (Cannat et al., 1992). The host rocks of these olivines are more-refractory peridotites than in the MARK region.

Orthopyroxene

Three main groups of orthopyroxene can be distinguished microscopically:

1. More or less rounded porphyroclasts (up to 10 mm long), with kink bands and clinopyroxene exsolution lamellae. Generally, the lamellae are partly, sometimes totally, transformed to serpentine. The outer rims are often replaced by talc and/or chrysotile.
2. Single grains (up to 2 mm diameter) within the matrix. The grains show undulatory extinction, kink banding, and contain very small clinopyroxene exsolutions.
3. Polygonal grain aggregates without deformation.

Orthopyroxene exsolution lamellae also occur in clinopyroxene.

A total of 74 prekinematic and postkinematic orthopyroxenes in thin sections from Hole 920 D was investigated using the electron microprobe (Table 5). The data show only small differences in Mg# (90.0–90.8), but they show a considerable variability of Al_2O_3 (3.5–4.9 wt%), Cr_2O_3 (0.55–1.15 wt%), and especially CaO (0.8–4.5 wt%) contents. TiO_2, MnO, and NiO contents also vary considerably.

No striking differences exist among the samples investigated, aside from the orthopyroxene in thin section 11 (Sample 920D-16R-6, Piece 10), in which the contents of Al_2O_3 and Cr_2O_3 are clearly higher.

Calculation of the quadrilateral molecular pyroxene proportions according to the International Mineralogical Association proposal (Morimoto et al., 1989) shows in the more or less "normal" orthopyroxene (n = 40; Mg# = 90.2, Ca# = 2.8, where Ca# = Ca/[Ca + Fe + Mg]):

Wollastonite (Wo) = 1.42–4.74 wt%, mean ($\bar{x}$) = 2.83, standard deviation (s) = ±0.95, V = ±33.6%
Enstatite (En) = 86.0–88.9 wt%, $\bar{x}$ = 87.60, s = ±0.91, V = ±1.04%
Ferrosilite (Fs) = 8.9–11.3 wt%, $\bar{x}$ = 9.57, s = ±0.37, V = ±3.87%.

A few orthopyroxenes with higher Wo proportions (n = 8; Mg# = 90.4, Ca# = 6.8) show the following:

Wo = 5.1–8.8 wt%, $\bar{x}$ = 6.81, s = ±1.44, V = ±21.1%
En = 82.2–85.7 wt%, $\bar{x}$ = 84.26, s = ±1.38, V = ±1.64%
Fs = 8.7–9.2 wt%, $\bar{x}$ = 8.93, s = ±0.166, V = ±1.86%

In both cases, standard deviation and variance are very low for En and Fs, but Wo varies over wide ranges. The orthopyroxenes richer in Wo show an increase in their Al_2O_3 content.

Table 4. Chemical composition of olivines from Hole 920D.

Sample no.:	10									
No.:	1	2	3	4	5	6	7	8	9	10
	Profile 1				Profile 2			Profile 3		
n:	1	2	1	2	1	2	3	1	1	1
SiO_2	41.82	41.59	41.46	40.92	41.41	41.37	41.23	41.25	41.10	41.18
TiO_2	0.01	–	–	–	–	–	–	–	–	–
Al_2O_3	0.02	0.02	–	0.03	0.02	0.02	0.03	0.01	0.02	0.01
Cr_2O_3	0.01	–	–	0.02	–	0.03	0.06	0.03	0.04	0.02
FeO	9.39	9.66	9.33	9.04	9.58	9.66	9.44	9.41	9.32	9.47
MnO	0.17	0.11	0.19	0.13	0.19	0.13	0.16	0.17	0.10	0.10
MgO	49.71	49.26	49.03	49.46	49.46	49.36	49.32	49.56	49.68	49.27
NiO	0.41	0.31	0.36	0.41	0.49	0.44	0.39	0.38	0.35	0.32
CaO	0.08	0.06	0.07	0.06	0.08	0.07	0.07	0.05	0.05	0.06
Total	101.62	101.01	100.44	100.07	101.23	101.08	100.70	100.86	100.66	100.43
Mg#	90.4	90.1	90.4	90.7	90.2	90.1	90.3	90.4	90.5	90.3
Fa	9.70	9.98	9.79	9.38	9.94	9.97	9.82	9.75	9.58	9.80
Fo	89.90	89.71	89.86	90.22	89.58	89.59	89.80	89.88	90.07	89.88
Nis	0.40	0.31	0.35	0.40	0.48	0.44	0.38	0.37	0.35	0.32

Sample no.:	10				11				12	
No.:	11	12	13	14	15	16	17	18	19	20
	Profile 4				Grain Profile				Grains	
n:	1	1	2	1	4	2	1	2	1	1
SiO_2	40.64	41.46	41.34	41.66	41.36	40.97	41.15	41.14	41.48	41.35
TiO_2	–	–	–	0.02	0.01	0.01	–	–	0.03	–
Al_2O_3	–	0.04	0.03	0.01	0.03	0.02	–	0.02	0.01	0.01
Cr_2O_3	–	–	0.02	0.02	0.02	0.01	–	–	–	0.02
FeO	9.91	9.25	9.11	9.47	9.42	9.58	9.28	9.61	9.35	9.56
MnO	0.18	0.17	0.13	0.15	0.12	0.10	0.09	0.17	0.15	0.18
MgO	49.47	48.70	49.35	49.63	49.47	49.05	49.35	49.73	49.46	48.92
NiO	0.41	0.30	0.35	0.32	0.41	0.37	0.39	0.42	0.38	0.29
CaO	0.02	0.05	0.03	0.02	0.06	0.06	0.06	0.04	0.02	0.04
Total	100.63	99.97	100.36	101.30	100.90	100.17	100.32	101.13	100.88	100.37
Mg#	89.9	90.4	90.6	90.3	90.3	90.1	90.4	90.2	90.4	90.1
Fa	10.23	9.77	9.43	9.64	9.72	9.93	9.59	9.89	9.70	10.03
Fo	89.37	89.93	90.25	90.01	89.87	89.70	90.03	89.70	89.93	89.68
Nis	0.40	0.30	0.32	0.35	0.41	0.37	0.38	0.41	0.37	0.29

Sample no.:	12					13				
No.:	21	22	23	24	25	26	27	28	29	30
	Grains		Profile			Grains				
n:	1	4	1	2	1	1	1	1	1	1
SiO_2	41.98	41.20	41.29	41.51	41.30	40.69	40.24	40.22	40.81	40.93
TiO_2	–	0.01	–	0.01	0.02	–	–	0.01	–	–
Al_2O_3	0.01	0.02	0.04	0.01	0.03	0.01	0.03	0.02	–	–
Cr_2O_3	0.01	0.01	–	–	–	0.03	–	–	–	0.02
FeO	9.11	9.68	9.70	9.50	9.73	9.38	9.60	9.54	9.41	9.46
MnO	0.06	0.14	0.14	0.13	0.11	0.17	0.10	0.11	0.11	0.12
MgO	49.62	49.17	49.45	49.59	49.53	49.22	49.68	49.77	49.09	49.17
NiO	0.43	0.40	0.35	0.38	0.39	0.43	0.43	0.38	0.39	0.37
CaO	0.02	0.04	0.05	0.04	0.05	0.03	0.04	0.03	0.03	0.02
Total	101.24	100.67	101.02	101.17	101.16	99.96	100.12	100.08	99.84	100.09
Mg#	90.7	90.0	90.1	90.3	90.1	90.3	90.2	90.3	90.3	90.3
Fa	9.36	10.03	10.01	9.76	9.99	9.78	9.83	9.78	9.77	9.82
Fo	90.22	89.57	89.65	89.86	89.63	89.80	89.75	89.85	89.84	89.81
Nis	0.42	0.40	0.34	0.38	0.38	0.42	0.42	0.37	0.39	0.37

Sample no.:	13		14			15					
No.:	31	32	33	34	35	36	37	38	39	40	41
	Profile		Grains					Profile			
n:	1	6	1	1	1	1	4	10	3	7	3
SiO_2	40.83	40.69	40.80	40.57	40.85	41.20	40.98	40.83	40.92	40.70	40.82
TiO_2	–	0.01	0.02	0.02	0.02	0.01	–	0.01	0.01	0.01	0.02
Al_2O_3	0.02	0.02	0.02	0.03	0.02	0.02	0.02	0.01	0.01	0.02	0.01
Cr_2O_3	0.02	0.01	0.03	0.05	–	0.03	0.01	0.01	–	–	–
FeO	9.25	9.50	9.27	9.26	9.07	9.21	9.55	9.54	9.44	9.64	9.42
MnO	0.12	0.13	0.15	0.13	0.14	0.15	0.14	0.12	0.15	0.14	0.15
MgO	49.04	49.21	49.50	49.13	48.85	49.88	49.35	49.16	49.69	49.18	49.25
NiO	0.39	0.41	0.32	0.34	0.46	0.41	0.42	0.40	0.41	0.41	0.42
CaO	0.02	0.03	0.02	0.03	0.03	0.01	0.01	0.03	0.02	0.03	0.05
Total	99.69	100.01	100.13	99.56	99.44	100.92	100.48	100.11	100.65	100.13	100.14
Mg#	90.4	90.2	90.5	90.4	90.6	90.6	90.2	90.2	90.4	90.1	90.3
Fa	9.65	9.86	9.62	9.66	9.52	9.50	9.88	9.90	9.73	10.00	9.79
Fo	89.97	89.75	90.06	90.00	90.02	90.10	89.71	89.71	89.87	89.60	89.79
Nis	0.38	0.39	0.32	0.34	0.46	0.40	0.41	0.39	0.40	0.40	0.42

Notes: No. = run number, *n* = number of analyses performed, Fo = forsterite, Fa = fayalite, Nis = Ni silicate ($Ni_2[SiO_4]$), – = not detected.

Table 5. Chemical composition of orthopyroxenes, Hole 920D (prekinematic and porphyroclastic grains).

Sample no.:	10	11								13
No.:	1	2	3	4	5	6	7	8	9	10
		Grains				Profile				Grain
n:	5	2	2	2	2	1	1	1	3	3
SiO_2	55.97	55.85	55.44	55.25	55.45	55.42	55.21	54.55	55.45	54.80
TiO_2	0.02	0.03	0.04	0.03	0.03	0.08	–	0.08	0.04	0.03
Al_2O_3	3.68	4.05	4.24	4.46	4.47	4.60	4.62	4.93	4.49	3.71
Cr_2O_3	0.76	0.92	1.02	1.00	0.99	1.06	1.15	1.03	0.98	0.73
FeO	6.09	6.05	6.02	6.34	6.41	6.24	5.83	5.73	6.33	6.23
MnO	0.16	0.17	0.16	0.16	0.14	0.15	0.13	0.09	0.14	0.16
MgO	32.68	32.46	32.16	32.67	32.58	31.75	31.12	30.01	32.65	32.90
NiO	0.11	0.11	0.11	0.12	0.14	0.15	0.10	0.12	0.10	0.08
CaO	1.63	1.66	1.37	0.73	0.86	2.12	2.57	4.48	1.18	1.18
Total	101.10	101.30	100.56	100.76	101.07	101.57	100.73	101.02	101.36	99.82
Mg#	90.5	90.5	90.5	90.2	90.0	90.1	90.5	90.3	90.2	90.4
Wo	3.14	3.21	2.68	1.42	1.67	4.13	5.08	8.81	2.28	2.26
En	87.48	87.41	87.85	88.68	88.38	86.16	85.72	82.25	87.95	88.14
Fs	9.38	9.38	9.47	9.90	9.95	9.71	9.20	8.94	9.77	9.60

Sample no.:	13									14
No.:	11	12	13	14	15	16	17	18	19	20
	Grains		Profile							Profile 1
n:	2	1	2	1	2	2	2	2	1	1
SiO_2	54.89	55.06	55.16	55.69	55.21	54.72	54.17	54.23	54.36	55.10
TiO_2	0.05	–	0.03	0.02	0.04	0.01	0.01	0.05	0.06	0.03
Al_2O_3	3.55	3.60	3.76	3.60	3.77	3.82	3.62	3.77	3.91	3.85
Cr_2O_3	0.69	0.55	0.74	0.73	0.78	0.86	0.68	0.78	0.84	0.76
FeO	5.76	6.35	6.14	6.25	6.16	6.37	6.28	6.09	5.68	6.26
MnO	0.15	0.16	0.13	0.14	0.11	0.13	0.12	0.12	0.11	0.17
MgO	31.76	32.81	32.63	33.43	32.98	32.98	32.78	31.76	30.60	32.62
NiO	0.08	0.18	0.09	0.05	0.16	0.08	0.11	0.08	0.09	0.09
CaO	2.43	1.40	1.80	0.84	1.06	0.81	1.24	2.32	4.26	1.60
Total	99.36	100.11	100.48	100.75	100.27	99.78	99.01	99.20	99.91	100.48
Mg#	90.8	90.2	90.4	90.5	90.5	90.2	90.3	90.3	90.6	90.3
Wo	4.74	2.68	3.45	1.61	2.04	1.56	2.39	4.52	8.29	3.07
En	86.26	87.58	87.16	88.86	88.53	88.65	87.99	86.05	82.91	87.29
Fs	9.00	9.74	9.39	9.53	9.43	9.79	9.62	9.43	8.80	9.64

Sample no.:	14										
No.:	21	22	23	24	25	26	27	28	29	30	31
	Profile 1				Profile 2					Profile 3	
n:	1	1	1	1	1	1	1	1	1	2	2
SiO_2	55.15	55.11	55.62	55.45	55.30	55.01	54.64	54.21	54.56	54.90	55.13
TiO_2	0.07	0.03	0.02	0.05	0.06	0.08	0.04	0.07	0.06	0.07	0.06
Al_2O_3	3.83	3.84	3.83	3.82	4.07	4.19	4.00	4.39	4.16	3.76	3.83
Cr_2O_3	0.75	0.73	0.70	0.72	0.88	0.90	0.87	0.94	0.96	0.82	0.77
FeO	6.15	5.76	5.96	6.12	6.37	6.12	5.95	5.72	5.92	5.80	6.21
MnO	0.16	0.13	0.13	0.18	0.12	0.15	0.17	0.14	0.17	0.07	0.18
MgO	32.90	30.97	32.86	32.87	32.42	32.71	31.73	30.77	32.23	31.74	32.85
NiO	0.05	0.17	0.09	0.13	0.12	0.06	0.12	0.12	0.19	0.10	0.11
CaO	1.10	4.16	1.07	1.06	1.33	0.98	2.32	3.66	2.14	2.80	1.07
Total	100.16	100.90	100.28	100.40	100.67	100.20	99.84	100.02	100.39	100.06	100.21
Mg#	90.5	90.6	90.8	90.5	90.1	90.5	90.5	90.5	90.7	90.7	90.4
Wo	2.12	8.01	2.08	2.05	2.57	1.91	4.52	7.16	4.13	5.42	2.07
En	88.37	83.14	88.71	88.46	87.60	88.57	86.17	83.89	86.70	85.70	88.33
Fs	9.51	8.85	9.21	9.49	9.83	9.52	9.31	8.95	9.17	8.88	9.60

Sample no.:	14				15						
No.:	32	33	34	35	36	37	38	39	40	41	42
	Profile 3				Profile				Grains		
n:	1	2	2	1	2	1	3	5	2	2	1
SiO_2	55.00	55.25	54.89	55.54	55.32	55.02	55.41	55.53	55.79	55.76	55.13
TiO_2	0.08	0.04	0.05	0.07	0.04	0.05	0.03	0.04	0.07	0.03	0.03
Al_2O_3	3.87	3.83	3.88	3.77	3.65	3.67	3.64	3.56	3.61	3.72	3.86
Cr_2O_3	0.72	0.76	0.84	0.65	0.80	0.77	0.73	0.72	0.76	0.75	0.86
FeO	5.89	6.20	5.73	6.06	6.24	5.90	6.26	6.39	6.26	6.14	6.05
MnO	0.05	0.18	0.11	0.13	0.15	0.15	0.14	0.15	0.12	0.13	0.19
MgO	32.03	32.73	31.92	32.94	32.43	31.60	32.75	32.70	32.48	32.58	31.83
NiO	0.13	0.08	0.09	0.09	0.10	0.13	0.11	0.09	0.14	0.09	0.17
CaO	2.11	1.23	2.42	1.14	1.45	2.94	1.36	1.34	1.71	1.68	2.16
Total	99.88	100.30	99.93	100.39	100.18	100.23	100.43	100.52	100.94	100.88	100.28
Mg#	90.6	90.4	90.9	90.6	90.2	90.5	90.3	90.1	90.2	90.4	90.4
Wo	4.10	2.37	4.71	2.20	2.81	5.68	2.62	2.58	3.29	3.24	4.20
En	86.87	88.02	86.42	88.48	87.52	85.19	87.77	87.60	87.13	87.34	86.33
Fs	9.03	9.61	8.87	9.32	9.67	9.13	9.61	9.82	9.58	9.42	9.47

Note: Abbreviations are defined in the text and in Table 4.

For both the orthopyroxene groups, no significant correlation between CaO/Cr_2O_3 and Al_2O_3/CaO could be calculated. On the other hand, Al_2O_3 and Cr_2O_3 are very strongly correlated:

orthopyroxene (n = 40): r = +0.875; (3.5% Al_2O_3)/(0.69% Cr_2O_3)–(5.0% Al_2O_3)/(1.14% Cr_2O_3),
orthopyroxene (n = 8): r = +0.883; (3.5% Al_2O_3)/(0.72% Cr_2O_3)–(5.0% Al_2O_3)/(1.12% Cr_2O_3).

High CaO and Al_2O_3/Cr_2O_3 contents in orthopyroxene can best be explained as the effects of high temperature in a dry system, only slightly influenced by pressure (Anastasiou and Seifert, 1972; Lindsley and Dixon, 1975; Obata, 1976; Sachtleben and Seck, 1981). Using the "Cr-Al-orthopyroxene" thermometer of Witt-Eickschen and Seck (1991), temperatures between 1245° and 1340°C, with an average of 1275°C, were calculated for 8 selected orthopyroxenes. The Lindsley (1983) two-pyroxene thermometer, applied to 8 orthopyroxene/clinopyroxene pairs, resulted in a range from 1250° to 1300°C, and even the "classic" Kretz (1963; 1982) two-pyroxene thermometer showed values between 1170° and 1380°C, with an average of ~1300°C. Only with the Wood and Banno (1973) method were higher temperatures (1450° ± 25°C) calculated.

Five grain profiles clearly show a tendency in the Fe and Mg distribution toward higher contents in the marginal zone and lower contents in the core. The inverse is true for Ni, to some degree. The behavior of Ca, Al, and Cr is irregular.

The microprobe results for a few polygonal grains and orthopyroxene exsolutions in clinopyroxene are listed in Table 6. The orthopyroxene exsolutions have a relatively wide range in Mg#s, as well as in the contents of Al_2O_3, FeO, NiO, and CaO. In contrast, however, the polygonal grains more or less correspond to the porphyroclastic orthopyroxenes, aside from their comparatively low CaO content.

A comparison with the data of Michael and Bonatti (1985) for orthopyroxenes from less-refractory and more-refractory peridotites from the northern section of the Mid-Atlantic Ridge shows a good correspondence between the mean value of all our orthopyroxenes and that from less-depleted peridotite; this is also consistent with the geochemical characteristics of MARK ultramafic rocks.

The orthopyroxene compositions of rocks from the 15°37′N region in the Mid-Atlantic Ridge axial valley (Cannat et al., 1992), which include strongly depleted peridotites, for instance, are clearly more refractory, with Mg# = 91.8 compared to a mean of Mg# = 90.2 in orthopyroxene from the Kane area.

Table 6. Chemical composition of orthopyroxenes, Hole 920D (postkinematic grains and exsolutions).

Sample no:	12		13			
No.:	43	44	45	46	47	48
	Polygonal grains		Exsolutions in clinopyroxene			
n:	3	3	1	1	1	1
SiO_2	56.06	56.34	53.53	54.69	54.62	54.99
TiO_2	0.03	0.04	0.02	0.03	0.07	0.07
Al_2O_3	3.53	3.63	5.20	3.74	3.86	3.79
Cr_2O_3	0.72	0.73	1.07	0.78	0.81	0.83
FeO	6.37	6.26	7.21	6.38	6.05	5.58
MnO	0.13	0.14	0.16	0.18	0.11	0.16
MgO	33.10	32.97	31.12	32.74	32.34	31.60
NiO	0.04	0.17	0.10	0.13	0.07	0.05
CaO	0.99	1.13	1.90	1.13	1.55	3.12
Total	100.97	101.41	100.31	99.80	99.48	100.19
Mg#	90.2	90.4	88.5	90.1	90.5	91.0
Wo	1.90	2.17	3.73	2.18	3.01	6.04
En	88.36	88.24	84.98	87.95	87.63	85.26
Fs	9.74	9.59	11.29	9.87	9.36	8.70

Note: Abbreviations are defined in text and Table 4.

Table 7. Chemical composition of clinopyroxenes, Hole 920D (prekinematic and porphyroclastic grains).

Sample no.:	10									11
No.:	1	2	3	4	5	6	7	8	9	10
	Grains			Profile						Profile
n:	4	2	1	3	2	2	3	2	1	2
SiO_2	52.04	52.42	51.82	52.15	52.36	52.02	51.83	51.93	52.45	51.47
TiO_2	0.07	0.13	0.11	0.08	0.07	0.09	0.10	0.12	0.11	0.19
Al_2O_3	4.67	4.45	4.59	4.64	4.61	4.75	4.91	4.74	4.85	5.75
Cr_2O_3	1.15	1.11	1.16	1.16	1.06	1.22	1.26	1.18	1.17	1.57
FeO	2.93	2.60	2.60	3.30	3.29	2.71	2.61	3.04	3.53	2.20
MnO	0.07	0.07	0.07	0.11	0.10	0.10	0.12	0.10	0.13	0.10
MgO	17.30	16.54	16.48	18.46	18.24	16.65	16.25	17.28	18.63	15.80
NiO	0.03	0.06	0.11	0.06	0.08	0.06	0.06	0.07	0.07	0.04
CaO	22.47	23.66	23.91	20.68	20.67	23.43	24.07	22.11	20.88	24.31
Na_2O	0.08	0.06	0.06	0.07	0.05	0.06	0.08	0.07	0.04	0.11
Total	100.81	101.10	100.91	100.71	100.53	101.09	101.29	100.64	101.86	101.54
Mg#	91.3	91.9	91.9	90.9	90.8	91.6	91.7	91.0	90.4	92.8
Ca*#	48.3	50.7	51.0	44.6	44.9	50.3	51.6	47.9	44.6	52.5
Wo	45.95	48.49	48.80	42.15	42.40	47.98	49.28	45.45	42.01	50.53
En	49.26	47.24	46.94	52.42	52.17	47.53	46.36	49.51	52.25	45.74
Fs	4.79	4.27	4.26	5.43	5.43	4.49	4.36	5.04	5.74	3.73

Sample no.:	11		12				13			
No.:	11	12	13	14	15	16	17	18	19	20
	Profile		Grains				Grains			
n:	6	2	3	2	1	1	2	2	3	3
SiO_2	51.31	50.94	51.33	51.82	52.27	52.21	50.65	50.33	50.61	51.34
TiO_2	0.15	0.16	0.10	0.10	0.07	0.08	0.09	0.08	0.10	0.13
Al_2O_3	5.51	5.73	5.03	5.02	4.68	5.01	4.98	5.11	4.46	4.57
Cr_2O_3	1.49	1.69	1.33	1.29	1.23	1.14	1.26	1.36	1.17	1.13
FeO	2.42	2.67	2.61	2.61	2.89	3.51	2.46	2.43	2.49	2.44
MnO	0.10	0.08	0.13	0.08	0.12	0.10	0.10	0.10	0.09	0.08
MgO	15.73	16.30	15.80	15.91	16.85	19.13	16.29	15.80	16.60	16.18
NiO	0.07	0.04	0.11	0.05	0.06	0.02	0.06	0.12	0.07	0.05
CaO	24.48	23.89	24.54	24.26	23.35	19.62	24.02	24.46	23.94	24.38
Na_2O	0.10	0.09	0.06	0.08	0.06	0.07	0.08	0.09	0.10	0.08
Total	101.36	101.59	101.04	101.22	101.58	100.89	99.99	99.88	99.63	100.38
Mg#	92.0	91.6	91.8	91.6	91.2	90.7	92.2	92.1	92.2	92.2
Ca*#	52.8	51.3	52.7	52.3	49.9	42.4	51.4	52.7	50.9	52.0
Wo	50.60	49.01	50.35	50.00	47.48	39.99	49.30	50.43	48.76	49.86
En	45.33	46.58	45.27	45.68	47.75	54.26	46.60	45.50	47.13	46.11
Fs	4.07	4.41	4.38	4.32	4.77	5.75	4.10	4.07	4.11	4.03

Clinopyroxene

Clinopyroxene is mainly developed as laminated porphyroclasts (up to 3–4 mm in size) with orthopyroxene exsolutions. Postkinematic recrystallization formed a smaller proportion of fresh and colorless grains, which are sometimes twinned, and occur subordinately in an intragranular position. They might represent products of a subsolidus crystallization process, but Nicolas et al. (1980) have discussed for that a formation by a limited local melting event. Exsolution lamellae in orthopyroxene constitute a third group of clinopyroxenes.

Microprobe data from 82, mainly prekinematic or synkinematic, clinopyroxenes are listed in Table 7, and show a range in Mg# from 90.0 to 92.8. These values are clearly greater than those from orthopyroxene. The high Al_2O_3 contents vary from 3.75 to 5.75 wt%, and are reflected by normative Ts (= tschermakite, Mg or Ca tschermakite) from 7.9% to 16.9%. The main components, CaO (19.1–24.7 wt%) and MgO (15.7–19.6 wt%), show a considerable variability, as do FeO (2.25–3.85 wt%) and Cr_2O_3 (0.85–1.7 wt%). Contents of the minor-element oxides TiO_2, MnO, NiO, and Na_2O vary quite substantially. The clinopyroxenes of thin section 11 (Sample 920D-16R-6, Piece 10) are distinguished by above average Al_2O_3 and Cr_2O_3 contents, as in the corresponding orthopyroxene. All clinopyroxenes in the samples investigated can be described as tschermakitic (chromian) diopsides.

The quadrilateral molecular pyroxene proportions, according to the IMA proposal (Morimoto et al., 1989), show a main group of clinopyroxenes with higher, and a subgroup with clearly lower Wo contents:

Main group (n = 33; Mg# = 91.6):

Wo = 46–50.6 wt%, $\bar{x}$ = 49.03, s = ±1.35, V = ±2.75%
En = 45.3–49.4 wt%, $\bar{x}$ = 46.71, s = ±1.22, V = ±2.61%
Fs = 3.7–4.8 wt%, $\bar{x}$ = 4.26, s = ±0.27, V = ±6.39%.

Subgroup (n = 12; Mg# = 90.6):
Wo = 38.6–45.5 wt%, $\bar{x}$ = 42.62, s = ±2.45, V = ±5.76%
En = 49.5–55.1 wt%, $\bar{x}$ = 52.01, s = ±2.07, V = ±3.98%
Fs = 4.8–6.3 wt%, $\bar{x}$ = 5.37, s = ±0.43, V = ±7.95%.

Standard deviations and variance for Wo and En are somewhat lower than for Fs, and the subgroup generally shows a greater compositional range. The clinopyroxene grains of this group show a dismemberment along cleavage planes and some dissolution features at these interruption zones, with the formation of antigorite, tremolite/actinolite, and, in some places, brown amphibole. This has led to a certain loss of Ca from the central parts of the grains, but the mean Al_2O_3 contents are nearly equal in both groups.

Peters (1968) has described a good correlation between Ca/(Ca + Mg) (defined as Ca*#, in Tables 7, 8) and the Al_2O_3 contents in clinopyroxene from Alpine serpentinites. The following correlations were calculated for the two clinopyroxene groups from Hole 920D:

clinopyroxene (n = 33): r = +0.481; Ca*# ranges from 46 at 3.94 wt% Al_2O_3 to 52 at 4.89 wt% Al_2O_3,
clinopyroxene (n = 12): r = –0.204; Ca*# ranges from 40 at 4.83 wt% Al_2O_3 to 48 at 4.63 wt% Al_2O_3.

This opposite behavior can be explained by the partial alteration of the clinopyroxene subgroup.

Al_2O_3 and Cr_2O_3 exhibit a positive correlation, but not as strong as that in the orthopyroxene system, and both groups differ noticeably:

Table 7 (continued).

Sample no.:	14			15						
No.:	21	22	23	24	25	26	27	28	29	30
	Grains			Profile			Grains			
n:	2	2	2	2	2	1	4	3	1	1
SiO_2	51.00	51.51	51.43	51.63	50.98	50.29	51.42	51.89	52.27	52.45
TiO_2	0.12	0.10	0.14	0.10	0.12	0.05	0.11	0.11	0.09	0.09
Al_2O_3	4.92	3.77	4.75	4.85	4.48	4.27	4.67	4.71	4.82	4.12
Cr_2O_3	1.37	0.87	1.13	1.24	1.21	1.13	1.28	1.18	1.26	1.19
FeO	2.42	2.74	2.54	2.61	2.39	2.71	2.46	2.39	2.46	2.67
MnO	0.07	0.13	0.10	0.13	0.08	0.07	0.10	0.07	0.05	0.10
MgO	16.02	16.92	17.27	15.93	15.92	16.78	15.94	16.05	16.68	17.42
NiO	0.04	0.06	0.08	0.06	0.07	0.08	0.07	0.04	0.11	0.08
CaO	24.12	23.53	22.57	24.50	24.72	23.98	24.69	24.58	23.50	22.80
Na_2O	0.08	0.08	0.09	0.11	0.12	0.13	0.11	0.13	0.13	0.11
Total	100.16	99.69	100.10	101.16	100.09	99.49	100.85	101.15	101.37	101.03
Mg#	92.2	91.7	92.4	91.6	92.2	91.7	92.0	92.3	92.4	92.1
Ca*#	52.0	50.0	48.4	52.5	52.7	50.7	52.7	52.4	50.3	48.5
Wo	49.86	47.69	46.33	50.17	50.61	48.39	50.49	50.31	48.21	46.29
En	46.12	47.78	49.43	45.46	45.44	47.23	45.43	45.75	47.77	49.31
Fs	4.02	4.53	4.24	4.37	3.95	4.38	4.08	3.94	4.02	4.40

Sample no.:	15						
No.:	31	32	33	34	35	36	37
				Grains			
n:	2	2	2	1	3	3	
SiO_2	52.19	51.30	51.41	50.99	51.81	51.39	51.67
TiO_2	0.12	0.10	0.12	0.11	0.09	0.10	0.11
Al_2O_3	5.18	5.20	5.10	5.16	4.44	5.02	4.65
Cr_2O_3	1.33	1.39	1.35	1.44	1.21	1.39	1.24
FeO	3.85	2.99	2.48	2.79	3.01	2.70	2.60
MnO	0.11	0.09	0.09	0.13	0.04	0.10	0.08
MgO	19.53	17.34	15.82	15.92	17.77	16.26	16.28
NiO	0.07	0.09	0.06	0.02	0.03	0.09	0.04
CaO	19.08	22.17	24.35	24.38	22.48	24.10	24.19
Na_2O	0.06	0.13	0.11	0.12	0.11	0.10	0.10
Total	101.52	100.80	100.89	101.06	100.99	101.25	100.96
Mg#	90.0	91.2	91.9	91.1	91.3	91.5	91.8
Ca*#	41.2	47.9	52.5	52.4	47.6	51.6	51.7
Wo	38.63	45.46	50.30	49.94	45.33	49.21	49.42
En	55.10	49.60	45.55	45.40	49.87	46.32	46.31
Fs	6.27	4.94	4.15	4.66	4.80	4.47	4.27

Note: Abbreviations are defined in Table 4 and in the text.

Table 8. Chemical composition of clinopyroxenes, Hole 920D (postkinematic grains and exsolutions).

Sample no.:	14		15					13
No.:	38	39	40	41	42	43	44	45
	Exsolutions in orthopyroxene			Postkinematic, intergranular				
n:	1	1	1	1	1	3	2	1
SiO_2	51.95	51.68	50.97	51.77	52.17	51.73	51.21	51.90
TiO_2	0.13	0.12	0.13	0.09	0.08	0.12	0.07	0.01
Al_2O_3	3.91	4.49	5.11	4.41	4.78	4.43	4.23	4.39
Cr_2O_3	0.99	1.15	1.34	1.13	1.20	1.16	1.07	1.10
FeO	2.25	2.48	2.70	3.33	3.25	2.88	3.00	3.45
MnO	0.08	0.10	0.08	0.11	0.09	0.10	0.07	0.08
MgO	16.69	16.39	16.13	18.90	18.13	17.31	17.58	19.65
NiO	0.04	0.03	0.11	0.09	0.15	0.08	0.10	–
CaO	24.29	23.97	23.83	20.56	21.78	23.02	22.25	19.65
Na_2O	0.08	0.05	0.14	0.08	0.08	0.10	0.09	0.08
Total	100.41	100.46	100.54	100.47	101.71	100.93	99.67	100.31
Mg#	93.0	92.2	91.4	91.0	90.9	91.4	91.3	91.0
Ca*#	51.1	51.3	51.5	43.9	46.3	48.8	47.6	41.8
Wo	49.22	49.12	49.11	41.44	43.81	46.52	45.25	39.51
En	47.10	46.76	46.42	53.13	50.95	48.78	49.87	54.95
Fs	3.68	4.12	4.47	5.43	5.24	4.70	4.88	5.54

Note: Abbreviations are defined in the text and in previous tables.

clinopyroxene (n = 33): r = +0.333; (3.5% Al_2O_3)/(0.83% Cr_2O_3)–(5.5% Al_2O_3)/(1.50% Cr_2O_3),
clinopyroxene (n = 12): r = +0.768; (3.5% Al_2O_3)/(0.89% Cr_2O_3)–(5.5% Al_2O_3)/(1.37% Cr_2O_3).

This mineral-chemical similarity could be the expression of compatible conditions during crystallization.

Three grain profiles demonstrate the opposite distribution of MgO and CaO: the rims are MgO rich and CaO poor, whereas the cores are MgO poor and CaO rich. FeO seems to follow the trend of MgO, but Al_2O_3, Cr_2O_3, and NiO show an indistinct behavior. The marginal decrease of CaO may be caused by aqueous fluids at higher temperatures, and the subsequent loss of a Ca-rich solution.

The correspondence between the chemical composition of the Kane clinopyroxene and the data of Michael and Bonatti (1985) for less-depleted peridotites is not very satisfactory, but the Mg# values lie close together (Kane: Mg# = 91.3; Michael and Bonatti [1985]: Mg# = 90.8). Clinopyroxene from more-refractory ultramafic rocks show Mg# values between 92.5 and 94 (Michael and Bonatti, 1985; Cannat et al., 1992). This is not surprising, when one considers the sensitivity of the relatively complex clinopyroxene system during partial melting, subsolidus, and hydration processes.

Some of the postkinematic intragranular clinopyroxenes (Table 8) exhibit relatively high Al_2O_3, Cr_2O_3, and FeO contents, as well as a lower TiO_2 content and nearly equal Mg#s, but low Ca*# values. These features are consistent with the formation of the postkinematic clinopyroxenes in a lower temperature regime than that of the prekinematic clinopyroxenes.

Only three exsolution lamellae were investigated. They all have low FeO but high CaO contents (high Ca*# values), and are relatively rich in TiO_2. The clinopyroxene exsolutions are enriched in TiO_2, Al_2O_3, and Cr_2O_3, in contrast with their host mineral, orthopyroxene. The lamellae are also somewhat enriched in MgO relative to FeO. Consequently, Mg# is slightly higher than it is in orthopyroxene. We can therefore state that clinopyroxene exsolution leads to a partial impoverishment of Ti, Mg, Cr, and Al in orthopyroxene. The composition of clinopyroxene exsolutions does not differ essentially from the composition of the prekinematic to synkinematic clinopyroxene, aside from some smaller Cr proportions.

Chromian Spinel

Cr spinel is an integral, but irregularly distributed, accessory mineral in ultramafic rocks. It occurs mostly as larger, lobate, but more or less fractured, grains in more or less altered olivines and orthopyroxenes. The grains always show some dissolution and commonly show a thin overgrowth of secondary magnetite, resulting from serpentinization. Results of a limited number of analyses from only three samples are compiled in Table 9, and the hypothetical mineral end members are calculated.

All grains investigated are picotites, with only small variances within individual thin sections. Spinels from sample 11 (Sample 920D-16R-6, Piece 10) are lower in Cr_2O_3 and somewhat higher in Al_2O_3 than those from sample 15 (Sample 920D-22R-2, Piece 1D). In thin section 11, the spinels show normative hercynite. Calculations for sample 15, however, result in magnesiochromite (MCm) and ferrochromite (Cm), with few exceptions. These differences do not support the opinions of Christiansen (1985) and Nicolas et al. (1980) about a metamorphic origin of both types of Cr spinel. Generally, the Cr spinels investigated are primary peridotite minerals, but in thin section 15 (Cr# >30, where Cr# = Cr/[Cr + Al]), a certain recrystallization at lower pressure should have modified the original composition, because the negative correlation between Cr# in spinel and Al_2O_3 in orthopyroxene is disturbed here. However, the two samples are not sufficient for a substantial statement to be made.

The mean element ratios for the Cr spinel groups are as follows (Fe^{3+}# = Fe^{3+}/[Fe^{3+} + Cr + Al]):

sample 11 (n = 11): Cr# = 28.3, Mg# = 67.6, Fe^{3+}# = 1.96,
sample 15 (n = 18): Cr# = 30.6, Mg# = 68.2, Fe^{3+}# = 1.37.

A geothermometric estimation of orthopyroxene-spinel pairs after equation 6 of Sachtleben and Seck (1981) gave ~1180°C for sample 11, and ~1075°C for sample 15. Both temperatures are lower than those calculated using pyroxene thermometry, and may reflect a certain element exchange between the spinels and the surrounding silicate minerals during subsolidus deformation and recrystallization.

OXYGEN-ISOTOPE INVESTIGATIONS FROM AN ULTRAMAFIC PROFILE, HOLE 920D: ALTERATION BY SEAWATER

Oxygen-isotope investigations from oceanic environments were first performed on samples dredged from the ocean floor (for example, Muehlenbachs and Clayton, 1971, 1972a, 1972b; Wenner and Taylor, 1973), and later on samples from borehole material (Muehlenbachs, 1976, 1977, 1978, 1979). The main results are the following: (1) Unaltered mid-ocean ridge basalt (MORB) samples give $\delta^{18}O$ = 5.7‰ ± 0.3‰ (i.e., $\delta^{18}O$ = 5.7‰ ± 0.2‰ from Muehlenbachs and Clayton, 1972a, 1972b; Kyser et al. 1982; Ito et al., 1987; for the bulk mantle $\delta^{18}O$ = 5.5‰, from Mattey et al., 1994). (2) Alteration pro-

Table 9. Chemical composition of Cr spinels, Hole 920D.

Sample no.:	11									
No.:	1	2	3	4	5	6	7	8	9	10
SiO_2	0.04	0.02	0.04	0.02	0.05	0.06	–	0.03	0.05	0.05
TiO_2	–	0.06	0.03	0.07	0.04	0.05	0.02	0.08	0.03	0.06
Al_2O_3	41.37	41.63	41.14	42.01	41.59	42.70	43.14	42.40	42.73	42.97
Cr_2O_3	24.87	24.48	25.10	25.08	25.36	24.12	24.83	24.15	24.96	25.44
Fe_2O_3	2.74	3.41	2.27	1.70	1.96	1.73	1.41	2.37	1.55	0.85
FeO	13.90	13.64	13.45	13.71	13.72	13.18	13.18	12.74	13.23	13.56
MnO	0.20	0.14	0.20	0.21	0.14	0.18	0.24	0.16	0.14	0.17
MgO	15.53	15.84	15.65	15.64	15.70	15.98	16.33	16.24	16.18	15.97
NiO	0.27	0.29	0.21	0.25	0.13	0.20	0.22	0.26	0.24	0.24
CaO	–	0.01	–	0.02	0.01	–	–	0.04	–	0.02
Total	98.91	99.49	98.07	98.69	98.70	98.20	99.37	98.47	99.10	99.32
Cr#	28.7	28.3	29.0	28.6	29.0	27.5	27.8	27.6	28.2	28.4
Mg#	66.6	67.4	67.5	67.0	67.1	68.4	68.8	69.4	68.6	67.7
Fe^{3+}#	2.92	3.61	2.44	1.82	2.09	1.84	1.48	2.52	1.64	0.89
Cm	27.95	27.36	28.42	28.20	28.57	27.13	27.45	27.12	27.80	28.35
MCm	–	–	–	–	–	–	–	–	–	–
Mt	2.93	3.62	2.44	1.82	2.10	1.84	1.48	2.53	1.64	0.90
Hc	2.68	1.61	1.85	3.11	2.36	2.83	2.47	0.98	2.06	3.13
Sp	66.44	67.41	67.29	66.87	66.97	68.20	68.60	69.37	68.50	67.62
Sample no.:	11	12	15							
No.:	11	12	13	14	15	16	17	18	19	20
SiO_2	0.04	0.04	0.01	0.07	0.03	0.07	0.08	0.06	0.05	0.03
TiO_2	0.05	0.01	0.07	0.05	0.08	0.09	0.09	0.05	0.05	0.11
Al_2O_3	42.72	41.38	41.48	41.25	41.28	40.96	41.17	41.13	41.11	41.54
Cr_2O_3	24.78	25.93	26.90	27.23	26.85	27.48	26.93	27.13	26.95	26.75
Fe_2O_3	1.26	2.26	1.58	1.62	1.75	1.37	1.65	1.70	1.52	1.59
FeO	13.26	12.23	13.57	13.32	13.01	13.13	12.91	12.72	13.15	12.84
MnO	0.15	0.15	0.17	0.13	0.16	0.19	0.15	0.20	0.14	0.12
MgO	16.04	16.67	16.03	16.15	16.19	16.07	16.14	16.28	16.15	16.34
NiO	0.19	0.23	0.18	0.18	0.33	0.20	0.32	0.31	0.13	0.30
CaO	0.02	–	–	–	–	–	0.02	0.07	–	–
Total	98.50	98.90	100.01	100.00	99.68	99.55	99.44	99.66	99.25	99.61
Cr#	28.0	29.6	30.3	30.7	30.4	31.0	30.5	30.7	30.5	30.2
Mg#	68.3	70.8	67.8	68.4	68.9	68.6	69.0	69.5	68.6	69.4
Fe^{3+}#	1.34	2.40	1.66	1.70	1.85	1.45	1.74	1.80	1.62	1.68
Cm	27.63	26.86	29.92	30.95	29.24	30.17	29.24	28.79	29.89	28.92
MCm	–	2.11	–	0.34	0.73	0.64	0.98	1.58	0.30	0.92
Mt	1.33	2.40	1.67	1.77	1.86	1.46	1.76	1.81	1.62	1.68
Hc	3.20	–	0.76	–	–	–	–	–	–	–
Sp	67.84	68.63	67.65	66.94	68.17	67.73	68.02	67.82	68.19	68.48
Sample no.:	15									
No.:	21	22	23	24	25	26	27	28	29	30
SiO_2	0.07	0.07	0.02	0.04	0.08	0.02	0.07	0.06	0.08	0.01
TiO_2	0.04	0.09	0.07	0.08	0.09	0.06	0.09	0.06	0.07	0.08
Al_2O_3	40.74	41.21	41.22	41.04	41.37	41.03	41.20	41.09	41.63	40.99
Cr_2O_3	27.13	26.87	27.52	27.19	26.79	26.89	26.91	27.03	26.81	27.29
Fe_2O_3	1.67	2.02	1.24	1.06	1.70	1.69	1.63	1.51	1.37	1.11
FeO	13.55	13.22	13.49	13.05	12.92	12.84	13.22	12.96	13.23	13.36
MnO	0.17	0.17	0.16	0.20	0.12	0.14	0.11	0.16	0.14	0.16
MgO	15.78	16.10	15.99	16.01	16.27	16.25	16.08	16.16	16.09	15.93
NiO	0.22	0.25	0.27	0.23	0.19	0.31	0.20	0.24	0.21	0.22
CaO	0.01	0.01	0.03	0.01	0.01	–	–	–	0.04	–
Total	99.36	100.00	100.01	98.91	99.54	99.21	99.51	99.26	99.67	99.14
Cr#	30.9	30.4	30.9	30.8	30.3	30.5	30.5	30.6	30.2	30.9
Mg#	67.5	68.4	67.9	68.6	69.2	69.3	68.4	69.0	68.4	68.0
Fe^{3+}#	1.78	2.13	1.32	1.13	1.80	1.79	1.72	1.59	1.44	1.18
Cm	30.50	29.49	30.67	30.35	29.06	28.93	29.86	29.52	30.00	30.64
MCm	–	0.53	–	0.19	0.94	1.16	0.30	0.79	–	–
Mt	1.78	2.15	1.32	1.13	1.82	1.80	1.74	1.60	1.45	1.18
Hc	0.34	–	0.21	–	–	–	–	–	0.19	0.27
Sp	67.38	67.83	67.80	68.33	68.18	68.11	68.10	68.09	68.36	67.91

Note: Abbreviations are defined in the text and in previous tables.

cesses by seawater at low temperatures (lower than 100°C) produces $\delta^{18}O > 5.7‰$, partly a strong O^{18} enrichment that depends on temperature and degree of alteration (whole-rock $\delta^{18}O$ up to more than 10‰, smectite up to more than 20‰, Muehlenbachs and Clayton, 1972a). Basalts show a correlation between $\delta^{18}O$ and water content. (3) Alteration processes by seawater at higher temperatures decrease the ^{18}O content. The latter is the case for seawater-formed serpentine minerals (Wenner and Taylor, 1971, 1973; Margaritz and Taylor, 1974; Ikin and Harmon, 1983; Tsen-Fu Yuei et al., 1990).

In this study, $\delta^{18}O$ was determined from samples of a harzburgitic serpentinite profile from Hole 920D. To separate relict minerals from each profile segment, samples with the lowest degree of alteration were selected. Insofar as possible, olivine, orthopyroxene, and clinopyroxene were separated, in addition to serpentine and spinel/magnetite.

All analyses were made in a nickel-glass line using ClF_3 to liberate oxygen, which was converted to CO_2, and measured in a delta E mass spectrometer. The $\delta^{18}O$ data are related to SMOW (standard mean ocean water), as National Bureau of Standards quartz no. 28 was used. All analyses were made in duplicate. The reproducibility was better than 0.2‰.

The $\delta^{18}O$ values are shown in Table 10. We note the following features:

1. The $\delta^{18}O$-values of the whole-rock samples decrease from the bottom of the profile (4.6‰) to the top (3.0‰).

Table 10. Oxygen-isotope data ($\delta^{18}O$) from harzburgites, Hole 920D.

Core, section, piece	Depth (mbsf)	Whole rock	Olivine	Orthopyroxene	Clinopyroxene	Serpentine	Magnetite
3R-1, 6	18.2	3.0		5.2	–	–	2.9
5R-1, 4	37.1	2.9			–	2.8	3.1
14R-4, 6	119.4	4.3	5.9	6.1	5.9	4.7	3.8
16R-1, 5D	134.4	3.8	6.1	6.1	6.1	4.2	3.0
19R-1, 5	162.7	3.3		6.0	–	3.2	–
20R-5, 4	177.6	4.0	6.1	6.1	5.9	3.7	3.1
21R-2, 5B	183.9	3.8	5.6	5.8	5.9	3.8	3.1
22R-4, 1B	192.1	4.6	5.5	5.9	5.8	5.3	3.6

Note: – = mineral fraction is not present.

2. The deepest sample 16 (Sample 920D-22R-4, Piece 1B) has a $\delta^{18}O$ distinctly smaller than the mean $\delta^{18}O$ value of fresh MORB (5.7‰). We conclude that all these whole-rock samples were altered by circulating ocean waters, and the lowered $\delta^{18}O$ values indicate that these ocean waters were heated.
3. This tendency toward lower ^{18}O contents is not uniform: the third sample from the top (sample 8: Sample 920D014R-4, Piece 6), has the second highest $\delta^{18}O$ (4.3‰), much higher than values from samples taken nearby. The third sample from the bottom (sample 13: Sample 920D-20R-5, Piece 4) has the next highest value, 4.0‰ (Fig. 1). Low ^{18}O contents (relative to those of their neighbors) are obtained from samples 14 (Sample 920D-21R-2, Piece 5B), 12 (Sample 920D-19R-1, Piece 5), and the top samples 6 (Sample 920D-5R-1, Piece 4), and 5 (Sample 920D-3R-1, Piece 6), which must indicate localities of rechanneled flow of ocean water (i.e., in fault zones). The mineral separates can be divided into a group of relict minerals including olivine, orthopyroxene, and clinopyroxene, and most of the spinel/magnetite, and another group of consisting of alteration products, mainly serpentine and traces of extremely fine-grained magnetite formed during the serpentinization.
4. The *primary* formed, relict minerals (olivine, orthopyroxene, clinopyroxene) almost all have similar $\delta^{18}O$, which is similar to MORB (5.7‰); they seem to be slightly enriched in ^{18}O in the middle part of the profile. At the top of the profile, the orthopyroxene (sample 5: Sample 920D-3R-1, Piece 6; $\delta^{18}O$ = 5.2‰) is distinctly lowered.
5. Of the *secondary* minerals, serpentine has a $\delta^{18}O$ range from 5.3‰ to 2.8‰, which is in the lower part of the range for oceanic serpentines reported by Tsen-Fu Yui et al. (1990; 3.0‰ to 12.4‰), and in the middle of the range reported by Wenner and Taylor (1973; +0.8‰ to 6.7‰).

Of all minerals investigated, serpentine $\delta^{18}O$ is most similar to whole-rock $\delta^{18}O$. The whole-rock $\delta^{18}O$ and the serpentine $\delta^{18}O$ are correlated (Fig. 1). The whole-rock peak of sample 8 (Table 1) is also conspicuous in the serpentine profile.

The spinel/magnetite $\delta^{18}O$ changes by only 0.9‰, and also exhibits a striking peak at the level of sample 8. Furthermore, two groups of samples have a constant $\delta^{18}O$ (within the measurement error of 0.2‰), one with 3.6‰ and 3.8‰, and the second from 2.9‰ to 3.1‰.

The difference (serpentine – spinel/magnetite) is very small and decreases from +1.7‰ to –0.3 ‰ (within the measurement error). Using the temperature calibration of Wenner and Taylor (1973) for ^{18}O in coexisting serpentine and magnetite, we get (also with the largest difference, 1.7‰) unreasonably high temperatures, effectively ∞. This means that our spinel/magnetite samples contain nearly no secondary magnetite, formed during serpentinization (in isotope-exchange equilibrium with serpentine).

The isotope pattern in Figure 2 shows an obvious trend between whole rock and serpentine, but a great difference between olivine, orthopyroxene, clinopyroxene, and spinel/magnetite, and the two groups of magnetite: (1) samples 8 and 16, mean $\delta^{18}O$ = 3.7‰, which are the least altered whole-rock samples; (2) samples 14, 10, 6, and 5, mean $\delta^{18}O$ = 3.0‰. Data from each group exhibit a surprisingly small degree of scatter.

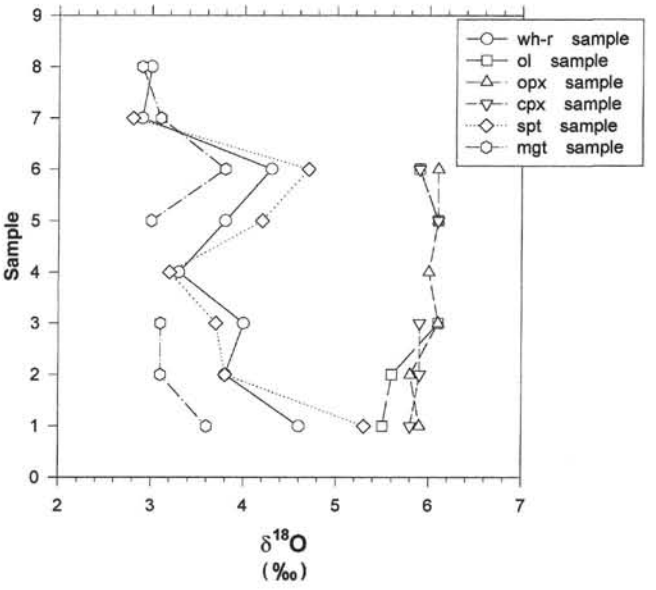

Figure 1. $\delta^{18}O$ vs. harzburgite profile. Sample 1 = Sample 153-920D-22R-4 (Piece 1B), sample 2 = Sample 153-920D-21R-2 (Piece 5B), sample 3 = Sample 153-920D-20R-5 (Piece 4), sample 4 = Sample 153-920D-19R-1 (Piece 5), sample 5 = Sample 153-920D-16R-1 (Piece 5D), sample 6 = Sample 153-920D-14R-4 (Piece 6), sample 7 = Sample 153-920D-5R-1 (Piece 4), and sample 8 = Sample 153-920D-3R-1 (Piece 6). Abbreviations are defined as follows: wh-r = whole-rock, ol = olivine, opx = orthopyroxene, cpx = clinopyroxene, spt = serpentinite, mgt = magnetite.

If these alterations are due to the influence of circulating, hot, and possibly acidic ocean waters, then a relation between $\delta^{18}O$ and some trace-element concentrations (especially of those trace elements that are more concentrated in the original ocean water) is possible. Figure 3 and Table 11 show a clearly negative correlation between whole-rock $\delta^{18}O$ and sulfur. In this regard, the results of sulfur-isotope analyses, which are in progress, may prove very exciting, because the ocean sulfate $\delta^{34}S$ of 20.3‰ is very different from the mantle value (near 0‰).

The relations with other elements are not as convincing (Table 11): boron seems to be enriched with increasing alteration, similar to sulfur, and is characterized by greater scatter. Chlorine seems to be impoverished with increasing alteration, and strontium exhibits no significant correlation with alteration.

The water content (expressed as LOI) shows no correlation with the whole-rock $\delta^{18}O$. Instead, we have two groups, containing exactly

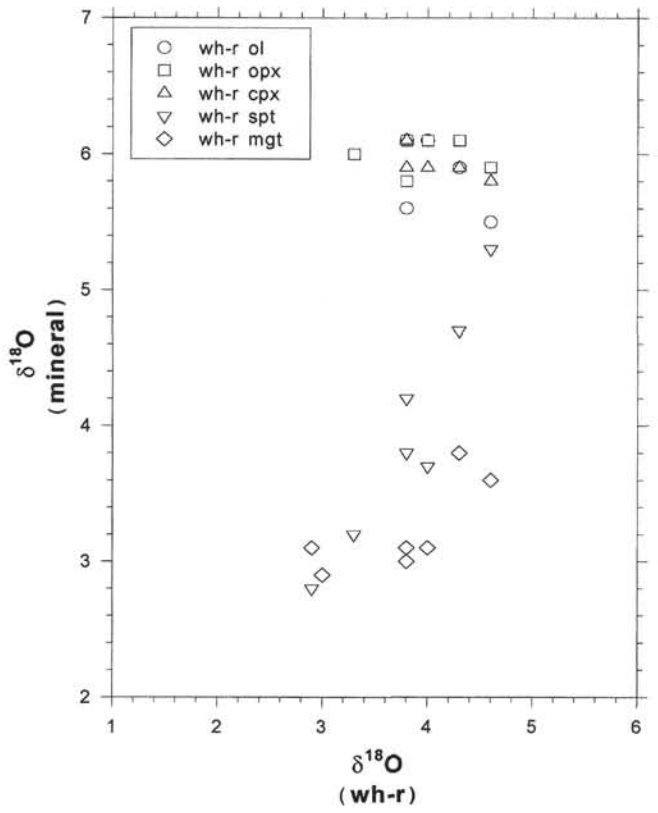

Figure 2. Whole-rock $\delta^{18}O$ values plotted vs. $\delta^{18}O$ values from different minerals. Alteration processes decreased whole-rock $\delta^{18}O$ values.The relict minerals olivine, clinopyroxene, and orthopyroxene (in contrast to serpentinite and magnetite) underwent almost no oxygen alteration in the different levels of the profile. Abbreviations are defined in Figure 1.

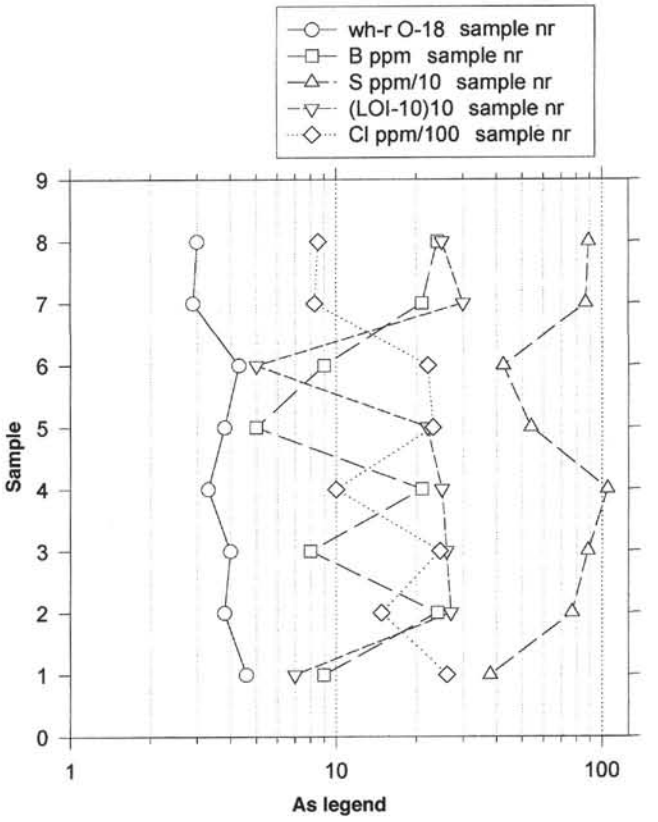

Figure 3. Whole-rock $\delta^{18}O$, B, S/10, LOI – 10, and Cl/10 plotted vs. the sample profile of harzburgites (see Fig. 1). The alteration seems to increase (in a different manner) with the contents of B, S, and Cl, and with LOI. Abbreviations are defined in Figure 1.

Table 11. Whole-rock $\delta^{18}O$ and the content of B, S/10, Cl/100, Sr, and (LOI – 10) · 10 from harzburgites, Hole 920D.

Core	Whole-rock $\delta^{18}O$	B (ppm)	S/10 (ppm)	(LOI – 10) · 10	Cl/100 (ppm)	Sr
3R	3.0	24	89.0	25	8.55	2.47
5R	2.9	21	87.0	30	8.30	0.93
14R	4.3	9	42.5	5	22.10	1.45
16R	3.8	5	54.0	22	23.10	1.21
19R	3.3	21	105.0	25	10.00	4.65
20R	4.0	8	88.5	26	24.55	2.28
21R	3.8	24	77.0	27	14.80	2.59
22R	4.6	9	38.0	7	26.10	2.47

the same samples as the two groups of magnetite $\delta^{18}O$: high magnetite $\delta^{18}O$ (3.7‰) is associated with low LOI, and vice versa. The difference in the LOI values is small.

Isotope Temperatures

Assuming isotope-exchange equilibrium, we have calculated isotope temperatures for the mineral pairs clinopyroxene (diopside) and magnetite (spinel). We used the relation of Bottinga and Javoy (1975) for anhydrous minerals for temperatures (T) higher than 500°C and the coefficient for these minerals given by Matthews et al. (1983):

$$\Delta^{18}O \text{ (clinopyroxene – magnetite)} = 4.03 \cdot 10^6/T^2$$

We get reasonable temperatures (Table 12), which cluster around 1100° and 900°C. However, one must consider that we do not have "pure" magnetite, but Cr spinel with a different composition, but the same crystal structure. Therefore, the calculation is affected by a partial uncertainty.

It is also difficult to obtain temperatures from the clinopyroxene-olivine pair. The olivine $\delta^{18}O$ values (Table 10) form two groups, and the group around 6.0‰ does not differ from the $\delta^{18}O$ of orthopyroxene and clinopyroxene. It is known that the $\delta^{18}O$ values of clinopyroxene and orthopyroxene at such high temperatures do not differ (Bottinga and Javoy, 1975). The lack of a difference between pyroxene and olivine raises the question whether, at this level, these minerals were formed in isotope-exchange equilibrium. Examples of coexisting minerals of oceanic samples with clear disequilibrium have been reported (Muehlenbachs and Clayton, 1971).

The two deepest samples, samples 16 (Sample 920D-22R-4, Piece 1B), and 14 (Sample 920D-21R-2, Piece 5B), have lower $\delta^{18}O$ in olivine, with a mean of 5.55‰; using the mean of orthopyroxene and clinopyroxene of 5.85‰, we get $\Delta^{18}O = 0.30$‰. (If we tentatively

Table 12. Calculated temperatures (T) for clinopyroxene-magnetite, for the formation of the serpentines using $\delta^{18}O = 0$ and final $\delta^{18}O$ of water equilibrated by formation of antigorite, Hole 920D.

Core, section, piece	Depth (mbsf)	T(°C) (cpx-mgt)	T(°C) (serpentine), $\delta^{18}O_W = 0$	$\delta^{18}O_W$ T = 235°C	$\delta^{18}O_W$ T = 250°C
3R-1, 6	18.2			–	–
5R-1, 4	37.1		≥183	1.45	1.80
14R-4, 6	119.4	1112	≥134	3.35	3.70
16R-1, 5D	134.4	867	≥146	2.85	3.20
19R-1, 5	162.7		≥171	1.85	2.20
20R-5, 4	177.6	927	≥158	2.35	2.70
21R-2, 5B	183.9	927	≥155	2.45	2.80
22R-4, 1B	192.1	1080	≥121	3.95	4.30
∅ group 1		1096			
∅ group 2		906			

Note: W = water, cpx = clinopyroxene, mgt = magnetite. ∅ group 1 = mean of Sample 14R-4, (Piece 6) and 22R-4 (Piece 1B); ∅ group 2 = mean of Samples 16R-1 (Piece 5D), 20R-5 (Piece 4), and 21R-2 (Piece 5B).

calculate a temperature with the relation and coefficient B = 1.240 of Bottinga and Javoy [1975], assuming an error of 0.2‰, we get a temperature of 1860°, with a variation between –450° and +1200°).

To calculate the isotope temperature of serpentinization, we need a second mineral, with a $\delta^{18}O$ value lower than that of serpentine, that formed in isotopic equilibrium with serpentine. Unfortunately, it was not possible to separate the very fine grained magnetite, which occurs only as traces and is intensively intergrown with serpentine. We tentatively calculated temperature, using the relation for serpentine-water from Wenner and Taylor (1971, 1973), and assuming $\delta^{18}O$ = 0.0‰ for water as an extreme case (Table 12). We obtained temperatures between 121° and 183°C, increasing from bottom to top! Wenner and Taylor (1971; 1973) estimated 125°C for lizardite and 180°C for chrysotile in Mid-Atlantic Ridge environments. Our samples, however, also contain antigorite (and some additional minerals, formed up to the transitional zone between greenschist and amphibolite facies). Wenner and Taylor (1971; 1973) estimated 225° and 235°C for antigorite. Pressure-temperature diagrams for the harzburgite system in equilibrium give a range from 250° to 550°C for antigorite at a pressure of 3 kbar (Bucher and Frei, 1994, p.153). We calculated the resulting $\delta^{18}O$ for water that has attained isotopic equilibrium with the forming antigorite, assuming temperatures of 235° and 250°C (Table 12), and obtained ranges from 1.45‰ to 3.95‰, and 1.80‰ to 4.30 ‰. The seawater with $\delta^{18}O$ = 0‰ had taken up ^{18}O by the formation of serpentine from olivine and other minerals.

Water/Rock Ratios

For the calculation of water/rock or better water/mineral (serpentine) ratios, we used the expressions of Taylor (1978). We assumed temperatures of 235°, 250°, and 300°C, and calculated ratios for closed and open systems in the sense of Taylor (Table 13). The final $\Delta^{18}O$ (serpentine – water) is calculated for these temperatures using the equation of Wenner and Taylor (1973). For the deepest sample, only a small amount of water was available and active. The higher the sample position within the profile, the more water could penetrate to that point and cause isotope exchange (and, of course, mineral reorganization).

CONCLUSIONS AND SUMMARY

The ultramafic rock samples investigated are serpentinized harzburgites that contain 15%–30% relict minerals. Whole-rock geochemistry shows the normal pattern of less-depleted, refractory mantle peridotites. Si, Mg, and Fe contents are very uniform, as are the compatible trace elements, but contents of K, Na, Ti, and especially Ca, vary considerably. Partial anatexis of the primary mantle material and hydrothermal metamorphism of the depleted rocks lead to these irregularities, especially for Ca.

The relict minerals olivine, orthopyroxene, and clinopyroxene show different morphological and genetic varieties, but their chemical compositions are relatively uniform within and between the individual samples, especially with respect to their Mg/Fe ratios (Mg#) (Table 14).

Synkinematic or prekinematic olivine (with Fo = 89.8%–90.6%) and orthopyroxene show nearly identical Mg#, but different NiO contents: in olivine, NiO = 0.39 wt% (0.29–0.49 wt%), and in orthopyroxene, NiO = 0.11 wt% (0.05–0.19 wt%). All these features are characteristic of less-refractory mantle minerals.

The contents of Al_2O_3 and Cr_2O_3 in orthopyroxene are strongly correlated (r = +0.88). CaO locally shows strikingly high concentrations (up to 4.5 wt%), leading to a subgroup with Wo contents between 5 and 8.8 wt%. Exsolution of clinopyroxene leads to a selective impoverishment of Ti, Mg, Cr, and Al in orthopyroxene.

The porphyroclastic clinopyroxene can be classified as tschermakitic diopside because of its high Al_2O_3 content (3.75–5.75 wt%). Al_2O_3 is well correlated with Cr_2O_3 in two groups (r_1 = +0.33; r_2 = +0.77), but not as strongly as in orthopyroxene. The general coincidence of these features with the equivalent data for orthopyroxene seems to reflect comparable conditions during the crystallization of both the pyroxenes. The behavior of Mg and Ca is clearly the opposite, and the scatter of Ca*#s is remarkable. Microprobe profiles through clinopyroxene grains show MgO-rich and CaO-poor rims, as well as MgO-poor and CaO-rich cores. The marginal decrease in CaO may be caused by reaction with fluids at higher temperatures, and probably also by partial melting.

In addition to the main group of clinopyroxenes (Wo = 49, En = 46.7, Fs = 4.3), a subgroup exists that is clearly poorer in Ca and richer in Mg (Wo = 2.6, En = 52, Fs = 5.4). Both groups differ strongly in the correlation between Ca*# and Al_2O_3: the Wo-rich group has r = +0.48, and the Wo-poor group has r = –0.20. This opposite behavior should be the result of partial alteration with a loss of Ca.

The chromian-bearing spinels are typical picotites, but with certain differences. Hercynite-bearing samples are slightly poorer in Cr_2O_3, grains with somewhat higher Cr_2O_3 contents show some Mg chromite by calculation. All Cr spinels investigated must be considered as primary constituents of the peridotite, but they are altered to some degree.

Different temperatures were calculated using several geothermometric methods:

1245°–1340°C, mean value = 1275°C ("Cr-Al-orthopyroxene" geothermometer; Witt-Eickschen and Seck, 1991),
1250°–1300°C (two-pyroxene geothermometer; Lindsley, 1983),
1170°–1380°C, mean value ≈ 1300°C (two-pyroxene geothermometer; Kretz, 1963, 1982),
1425° ± 25°C (Wood and Banno, 1973).

Aside from the Wood and Banno (1973) data, the temperature ~1300°C may reflect the primary formation of prekinematic to synkinematic orthopyroxene and clinopyroxene in the protolith at pressures not greater than 10 kbar (Anastasiou and Seifert, 1972; Wyllie, 1981).

In the orthopyroxene-chromian spinel system, applying the method of Sachtleben and Seck (1981) on the basis of X_{Mg}, X_{Al}, and X_{Cr}, the two Cr-spinel-bearing samples yield temperatures of 1180° and 1075°C, respectively. With a certain restriction, the temperature estimate for the clinopyroxene-spinel/magnetite pair, using ^{18}O exchange, gave 1100° and 900°C. All these values may reflect subsolidus deformation and recrystallization processes, possibly in more than a single step.

Table 13. Calculated water/rock ratios for serpentine for closed and open systems for different temperatures, Hole 920D.

Core, section, piece	Depth (mbsf)	$(w/r)_{cs}$ T = 235°C	$(w/r)_{os}$ T = 235°C	$(w/r)_{cs}$ T = 250°C	$(w/r)_{os}$ T = 250°C	$(w/r)_{cs}$ T = 300°C	$(w/r)_{os}$ T = 300°C
3R-1, 6	18.2	–	–	–	–	–	–
5R-1, 4	37.1	(3.67)	(1.96)	(2.95)	(1.72)	(1.93)	(1.29)
14R-4, 6	119.4	0.61	0.53	0.56	0.48	0.44	0.39
16R-1, 5D	134.4	1.14	0.88	1.02	0.80	0.79	0.65
19R-1, 5	162.7	(2.69)	(1.62)	(2.26)	(1.44)	(1.58)	1.12
20R-5, 4	177.6	1.75	1.21	1.52	1.09	1.13	0.87
21R-2, 5B	183.9	1.26	0.94	1.10	0.85	0.82	0.67
22R-4, 1B	192.1	0.09	0.08	0.08	0.08	0.07	0.06

Notes: Numbers in parentheses represent values from serpentine with low $\delta^{18}O$, – = not calculable, w/r = water/rock ratio, cs = closed, os = open.

Table 14. Variation of mineral chemistry in the profile of Hole 920D.

			Olivine		Orthopyroxene		Clinopyroxene		
Sample no.	Core, section, piece	Depth (mbsf)	*n*	Mg#	*n*	Mg#	*n*	Mg#	Ca#
10	16R-1, 5D	134.4	20	90.33	5	90.53	20	91.29	48.26
11	16R-6, 6	140.3	9	90.27	14	90.28	10	92.08	52.47
12	19R-1, 5	162.7	11	90.19	–	–	7	91.34	50.75
13	20R-5, 4	177.6	12	90.29	18	90.42	10	92.18	51.87
14	21R-2, 5B	183.9	6	90.35	20	90.53	6	92.06	50.13
15	22R-2, 1D	192.1	28	90.21	16	90.26	29	91.60	50.82

Note: Symbols and abbreviations are defined in previous tables.

The $\delta^{18}O$ values are very uniform in the relict minerals olivine, orthopyroxene, and clinopyroxene, and values are similar to those of MORB, although slightly higher than for the bulk mantle. Whole-rock samples, serpentine, and magnetite show clearly lower $\delta^{18}O$ values, resulting from hydrothermal alteration at relatively high temperatures. The temperature determination of the serpentinization is restricted because only serpentine is available. Using some calculations and estimations about the water/rock ratio, a temperature range of ±250°C could be probable.

ACKNOWLEDGMENTS

We are grateful to the Deutsche Forschungsgemeinschaft, Bonn, for considerable financial support of this work. H.-J. Bernhardt (Bochum) has greatly supported the microprobe investigations, B. Knipping (Clausthal), and G. Bombach, E. Rüdiger, and K. Volkmann (Freiberg) were responsible for the analytical procedure. C.-D.W. is grateful to all these colleagues and their institutions. The nickel-glass line was constructed, and the samples were separated and prepared by W. Tikhomirov; the mass spectrometric analyses were performed by R. Liebscher. For critical reviews and constructive comments, we thank E. Bonatti, J. Karson, and especially P. Kelemen and B. Wathen.

REFERENCES

Anastasiou, P., and Seifert, F., 1972. Solid solubility of Al_2O_3 in enstatite at high temperatures and 1–5 kb pressure. *Contrib. Mineral. Petrol.*, 34:272–287.

Aumento, F., and Loubat, H., 1971. The Mid-Atlantic Ridge near 45°N. XVI. Serpentinized ultramafic intrusions. *Can. J. Earth Sci.*, 8:631–663.

Bottinga, Y., and Javoy, M., 1975. Oxygen isotope partitioning among the minerals in igneous and metamorphic rocks. *Rev. Geophys. Space Phys.*, 20:250–265.

Bucher, K., and Frei, M., 1994. *Petrogenesis of Metamorphic Rocks:* Berlin (Springer-Verlag).

Cannat, M., Bideau, D., and Bougault, H., 1992. Serpentinized peridotites and gabbros in the Mid-Atlantic Ridge axial valley at 15°37′N and 16°52′N. *Earth Planet. Sci. Lett.*, 109:87–106.

Cannat, M., Karson, J.A., Miller, D.J., et al., 1995. *Proc. ODP, Init. Repts.*, 153: College Station, TX (Ocean Drilling Program).

Cannat, M., and ODP Shipboard Scientific Party, 1995. Probing the foundation of the Mid-Atlantic Ridge. *Eos,* 76:129–133.

Christiansen, F.G., 1985. Deformation fabric and microstructures in ophiolitic chromitites and host ultramafics, Sultanate of Oman. *Geol. Rundsch.,* 74:61–76.

Dick, H.J.B., Fisher, R.L., and Bryan, W.B., 1984. Mineralogic variability of the uppermost mantle along mid-ocean ridges. *Earth Planet. Sci. Lett.,* 69:88–106.

Hamlyn, P.R., and Bonatti, E., 1980. Petrology of mantle-derived ultramafics from the Owen fracture zone, Northwest Indian Ocean: implications for the nature of the oceanic upper mantle. *Earth Planet. Sci. Lett.,* 48:65–79.

Hofmann, A.W., 1988. Chemical differentiation of the Earth: the relationship between mantle, continental crust, and oceanic crust. *Earth Planet. Sci. Lett.,* 90:297–314.

Ikin, N.P., and Harmon, R.S., 1983. A stable isotope study of serpentinization and metamorphism in the Highland Border suite, Scotland, U.K. *Geochim. Cosmochim. Acta,* 47:153–167.

Ito, E., White, W.M., and Göpel, C., 1987. The O, Sr, Nd and Pb isotope geochemistry of MORB. *Chem. Geol.,* 62:157–176.

Karson, J.A., and Winters, A.T., 1992. Along-axis variations in tectonic extension and accommodation zones in the MARK area, Mid-Atlantic Ridge 23°N latitude: ophiolites and their modern oceanic analogues. *In* Parsons, L.M., Murton, B.J., and Browning, P. (Eds.), *Ophiolites and Their Modern Oceanic Analogues.* Geol. Soc. Spec. Publ. London, 60:107–116.

Kretz, R., 1963. Distribution of magnesium and iron between orthopyroxene and calcic pyroxene in natural mineral assemblages. *J. Geol.,* 71:773–785.

————, 1982. Transfer and exchange equilibria in a portion of the pyroxene quadrilateral as deduced from natural and experimental data. *Geochim. Cosmochim. Acta,* 46:411–421.

Kyser, T.K., O'Neil, J.R., and Carmichael, I.S.E., 1982. Genetic relations among basic lavas and ultramafic nodules: evidence from osygen isotope compositions. *Contrib. Mineral. Petrol.,* 81:88–102.

Lindsley, D.H., 1983. Pyroxene thermometry. *Am. Mineral.,* 68:477–493.

Lindsley, D.H., and Dixon, S.A., 1975. Diopside-enstatite equilibria at 850° to 1,400°C, 5 to 35 kbar. *Am. J. Sci.,* 276:1282–1301.

Margaritz, M., and Taylor, H.P., Jr., 1974. Oxygen and hydrogen isotope studies of serpentinization in the Troodos ophiolite complex, Cyprus. *Earth Planet. Sci. Lett.,* 23:8–14.

Mattey, D., Lowry, D., and Macpherson, C., 1994. Oxygen isotope composition of mantle peridotite. *Earth Planet. Sci. Lett.*, 128:231–241.

Matthews, A., Goldsmith, J.R., and Clayton, R.N., 1983. Oxygen isotope fractionations involving pyroxenes: the calibration of mineral-pair geothermometers. *Geochim. Cosmochim. Acta*, 47:631–644.

Michael, P.J., and Bonatti, E., 1985. Peridotite composition from the North Atlantic: regional and tectonic variations and implications for partial melting. *Earth Planet. Sci. Lett.*, 73:91–104.

Miyashiro, A., Shido, F., and Ewing, M., 1969. Composition and origin of serpentinites from the Mid-Atlantic Ridge, 24° and 30°N latitude. *Contrib. Mineral. Petrol.*, 23:117–127.

Morimoto, N., et al., 1989. Nomenclature of pyroxenes. *Can. Mineral.*, 27:143–156.

Muehlenbachs, K., 1976. Oxygen isotope geochemistry of DSDP Leg 34 Basalts. *In* Yeats, R.S., Hart, S.R., et al., *Init. Repts. DSDP*, 34: Washington (U.S. Govt. Printing Office), 337–339.

————, 1977. Oxygen isotope geochemistry of rocks from DSDP Leg 37. *Can. J. Earth Sci.*, 14:771–776.

————, 1978. Oxygen isotope geochemistry of rocks from Leg 46. *In* Dmitriev, L., Heirtzler, J., et al., *Init. Repts. DSDP*, 46: Washington (U.S. Govt. Printing Office), 257–258.

————, 1979. The alteration and aging of the basaltic layer of the sea floor: oxygen isotope evidence from DSDP/IPOD Leg 51, 52, and 53. *In* Donnelly, T., Francheteau, J, Bryan, W., Robinson, P., Flower, M., Salisbury, M., et al., *Init. Repts. DSDP*, 51, 52, 53: Washington (U.S. Govt. Printing Office), 1159–1167.

Muehlenbachs, K., and Clayton, R.N., 1971. Oxygen isotope ratios of submarine diorites and their constitutent minerals. *Can. J. Earth Sci.*, 8:1591–1595.

————, 1972a. Oxygen isotope studies of fresh and weathered submarine basalts. *Can. J. Earth Sci.*, 9:172–184.

————, 1972b. Oxygen isotope geochemistry of submarine greenstones. *Can. J. Earth Sci.*, 9:471–478.

————, 1976. Oxygen isotope composition of the oceanic crust and its bearing on seawater. *J. Geophys. Res.*, 81:4365–4369.

Nicolas, A., Boudier, F., and Bouchez, J.L., 1980. Interpretation of peridotite structures from ophiolitic and oceanic environments. *Am. J. Sci.*, 280:192–210.

Obata, M., 1976. The solubility of Al_2O_3 in orthopyroxenes in spinel and plagioclase peridotites and spinel pyroxenite. *Am. Mineral.*, 61:804–816.

Peters, T., 1968. Distribution of Mg, Fe, Ca and Al in coexisting olivine, orthopyroxene and clinopyroxene in the total serpentinite (Davos, Switzerland) and in the Alpine metamorphosed Malenco serpentinite (N. Italy). *Contrib. Mineral. Petrol.*, 18:65–75.

Purdy, G.M., and Detrick, R.S., 1986. Crustal structure of the Mid-Atlantic Ridge at 23°N from seismic refraction studies. *J. Geophys. Res.*, 91:3739–3762.

Sachtleben, T., and Seck, H.A., 1981. Chemical control of Al-solubility in orthopyroxene and its implication on pyroxene geothermometry. *Contrib. Mineral. Petrol.*, 78:157–165.

Taylor, H.P., Jr., 1978. Oxygen and hydrogen isotope studies of plutonic granitic rocks. *Earth Planet. Sci. Lett.*, 38:177–210.

Wenner, D.B., and Taylor, H.P., 1973. Oxygen and hydrogen isotope studies of the serpentinization of ultramafic rocks in oceanic environments and continental ophiolitic complexes. *Am. J. Sci.*, 273:202–239.

Wenner, D.B., and Taylor, H.P., Jr., 1971. Temperatures of serpentinization of ultramafic rocks based on $^{16}O/^{18}O$ fractionation between coexisting serpentine and magnetite. *Contrib. Mineral. Petrol.*, 32:165–185.

Witt-Eickschen, G., and Seck, H.A., 1991. Solubility of Ca and Al in orthopyroxene from spinel peridotite: an improved version of an empirical thermometer. *Contrib. Mineral. Petrol.*, 106:431–439.

Wood, B.J., and Banno, S., 1973. Garnet-orthopyroxene and orthopyroxene-clinopyroxene relationships in simple and complex systems. *Contrib. Mineral. Petrol.*, 42:109–124.

Wyllie, P.J., 1981. Plate tectonics and magma genesis. *Geol. Rundsch.*, 70:128–153.

Yui, T.-F., Yeh, W.-H., and Lee, C.W., 1990. A stable isotope study of serpentinization in the Fengtien ophiolite, Taiwan. *Geochim. Cosmochim. Acta*, 54:1417–1426.

Date of initial receipt: 24 August 1995
Date of acceptance: 27 February 1996
Ms 153SR-018